COMPARISON OF EXPERIMENTAL NMR MEASUREMENTS WITH SIMULATED RESPONSES ON DIGITIZED IMAGES OF MONO-MINERALIC ROCKS USING XRAY-CT

C.H. Arns[1], Y. Melean[2], L. Burcaw[3], P.T. Callaghan[3], K.E. Washburn[4]
(1) School of Petroleum Engineering, University of New South Wales, Sydney, Australia
(2) Applied Maths, RSPhysSE, Australian National University, Canberra, Australia
(3) School of Chemical and Physical Sciences, Victoria University of Wellington, Wellington, New Zealand
(4) Weatherford Reservoir Laboratories Trondheim, Norway

This paper was prepared for presentation at the International Symposium of the Society of Core Analysts held in Noordwijk, The Netherlands 27-30 September, 2009

ABSTRACT

Nuclear magnetic resonance relaxation measurements in porous reservoir rocks are often used to produce 'pseudo-pore size' distributions of the systems. These are commonly correlated with mercury injection capillary pressure data, allowing estimation of a constant surface relaxivity for the NMR measurements. However, this approach is not an accurate comparison as the mercury injection measures pore space accessibility at a given pressure and produces a distribution of pore throat size as opposed to pore body size.

In this paper we ignore mineralogy effects and use a combination of Xray-CT and other methods to characterize the pore structure in 3D from tens of nanometers to centimeters. This work improves upon previous Xray-CT based simulations, where a surface relaxivity matching to experiment could take very high values (up to 50 micron/s) because the surface area measured from Xray-CT significantly underestimated the surface area reference measurement used to derive experimental surface relaxivities. We increase the discretisation in the numerical approach to about 100nm, giving a more accurate calculation of surface area and thus leading to a smaller surface relaxivity in the simulations. Our method also improves on previous models by calculating the internal magnetic fields produced within the rocks when subjected to an external magnetic field separately from the surface relaxivity. This allows us to model the dephasing explicitly based on structure and susceptibility contrast. Thus, a coarse scale voxel in a simplistic NMR simulation is replaced with a high-resolution model of structure, and the dependence on surface relaxivity is reduced since two fine-scale mechanisms contribute to the previously used single scale surface relaxivity.

To validate our modeling approach, the simulated NMR responses from the X-Ray CT images were compared with experimental NMR measurements on the mono-mineralic carbonate rocks. As the surface relaxivity parameter and internal magnetic fields produced by the samples are known to have dependence on the applied magnetic field strength, the relaxation responses were measured and simulated for low and high NMR frequencies.

INTRODUCTION

It has long been realised that the NMR T_2 relaxation response in reservoir rock is influenced by internal gradients, resulting from the susceptibility difference and spatial distribution of constituent materials, in addition to surface relaxation and restricted diffusion effects (Hürlimann 1998; Shafer et al., 1999; Dunn 2001; Dunn et al., 2001). When it is assumed that internal gradient effects are negligible, the magnetisation decay is fitted by a multi-exponential decay

$$M(t) = M_0(t)\sum_{p=1}^{N} a_p \exp\left[-\frac{t}{T_{2p}}\right] \quad , \tag{1}$$

where each pore p is assumed to be in the fast diffusion limit and T_{2p} is the relaxation time in an individual pore. A pore size distribution can then be calculated by taking

$$\frac{1}{T_{2p}} = \frac{1}{T_{2b}} + \rho\frac{S_p}{V_p} \quad , \tag{2}$$

with S_p and V_p being the surface area and volume of pore p, respectively. T_{2b} is the bulk relaxation time, and ρ the surface relaxivity. In this interpretation of the NMR response, the surface relaxivity becomes a fitting parameter dependent on the resolution and type of the surface area reference measurement; the distribution is shifted or "anchored" to overlap with a reference distribution, e.g. derived from mercury intrusion capillary pressure data. If internal gradients are not negligible, such a match is achieved for a particular magnetic field strength and temperature/diffusion coefficient and dephasing effects stemming from internal gradients are folded into bulk and surface relaxivity. It would be desirable to separate the influence of internal gradients from actual bulk fluid or surface relaxation. Attempts to decouple those effects have been made (Hürlimann 1998; Shafer et al., 1999). However, it is not a trivial problem and for complex multi-scale rocks a numerical approach is logical. An accurate representation of the microstructure of the sample is needed and is typically acquired using Xray-CT imaging (Arns et al., 2005; Arns et al. 2007). For micro-porous carbonates, the smallest scale cannot be resolved in 3D with a reasonable field of view, yet cannot be ignored due to coupling with macro-porosity. Several modelling approaches exist in literature for specific carbonate rocks (Crossley et al., 1991; Biswal et al., 2007; Wu et al., 2008). Here we use Crossley's approach by fitting a 2-point correlation function to micro-porous regions, using analytic expressions for Gaussian random fields (Roberts 1997; Arns et al., 2004).

METHODOLOGY

Sample characterisation and image processing

In this study we consider two vuggy carbonate rock samples from the Middle-East (see Fig. 1). We acquired tomographic images at about 3μm resolution for both samples to resolve larger scale heterogeneity (5mm diameter plug), and SEM images at two different resolutions to resolve length scales below Xray-CT resolution down to 200nm resolution for sample A, and 100nm resolution for sample B. Both samples contain a significant amount of micro-porosity and exhibit a bi-modal pore accessibility radius distribution based on mercury intrusion measurements (see Fig. 2). Since micro- and macro-porosity couple, a 3D structural model of the micro-porosity is needed for simulating the NMR response.

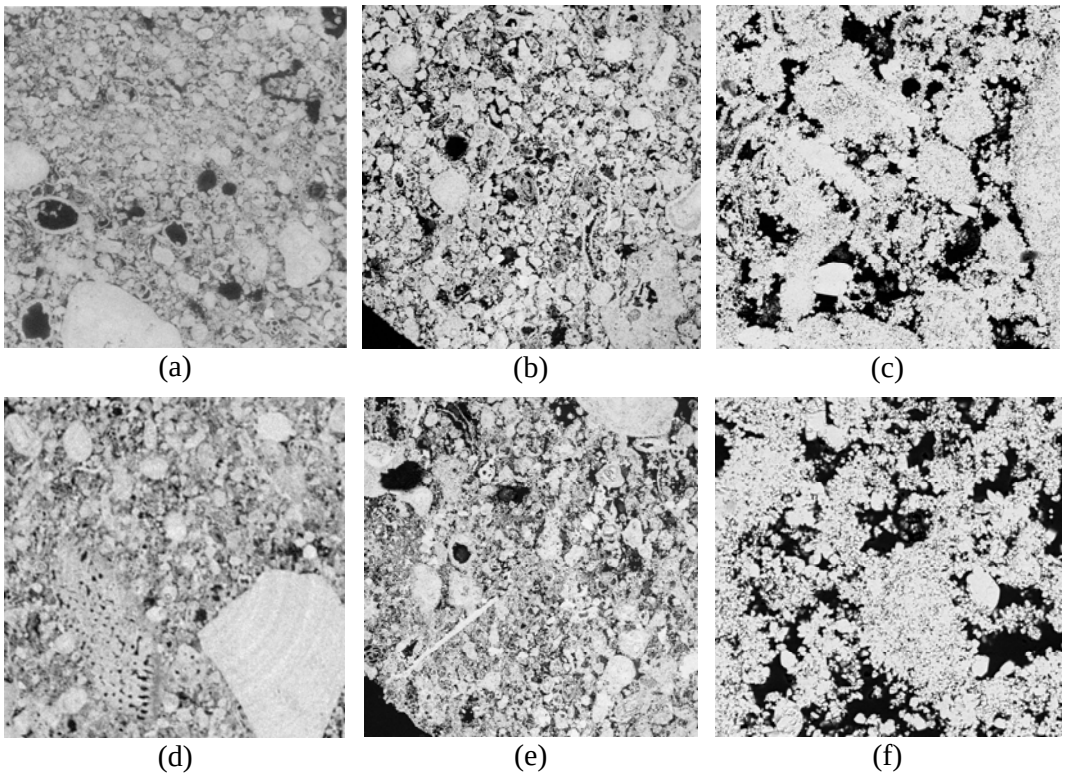

Fig. 1: Xray-CT slices and SEM images of the two carbonate cores considered in this study. Top: sample A, (a) Xray density slice through the tomogram at 2.56μm resolution and a field of view (FOV) of $(2.56mm)^2$, (b) SEM at 40x magnification, equaling 1.25μm pixel size, FOV=$(2.4mm)^2$ (c) SEM at 250x magnification or 200nm pixel size, FOV=$(0.384mm)^2$. Bottom: sample B, (d) Xray density slice through the tomogram at 2.86μm resolution, FOV=$(2.86mm)^2$, (e) SEM at 40x magnification, equaling 1.25μm pixel size, FOV=$(2.4mm)^2$, (f) SEM at 500x magnification or 100nm pixel size, FOV=$(0.192mm)^2$.

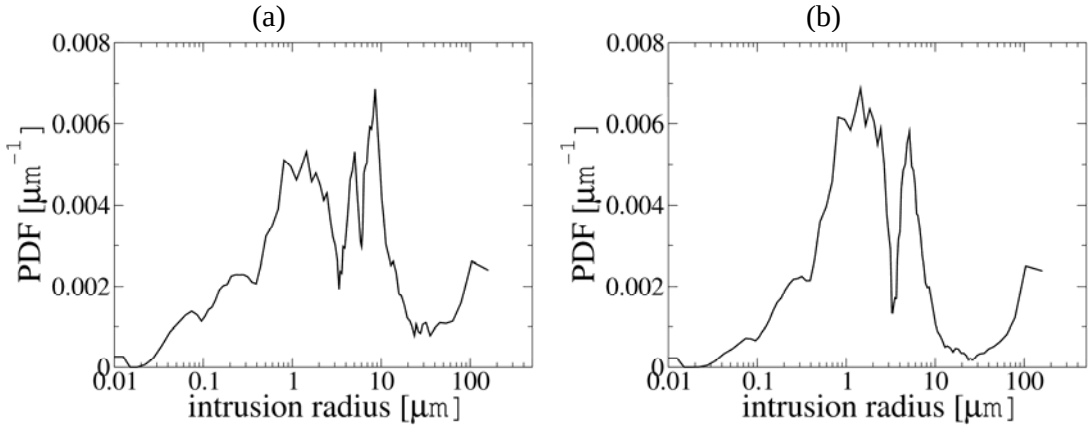

Fig. 2: Mercury intrusion capillary pressure measurements of samples A (left) and B (right) of this study, converted to saturation change versus pore accessibility radius (as probability density). Both samples exhibit a bi-modal pore accessibility radius distribution. The small peak at large radii is likely due to boundary effects and indicates the amount of larger pores accessible directly from the sample surface.

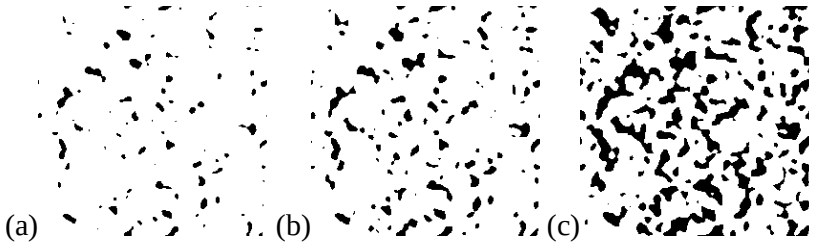

Fig. 3: Model microstructure for the micro-porous regions of the tomographic images shown in Fig. 1(a,d). Each 10^3 voxels of the tomogram correspond to 250^3 voxels of the model structure.

NMR measurements

The NMR experiments were carried out on a Bruker widebore 400 MHz Avance II spectrometer using the 5mm diameter samples imaged on the Xray-CT system. Both samples were saturated with brine and the NMR T_2 CPMG response measured under ambient conditions for a set of echo spacings. The same measurements were carried out at low field on a 2Mhz Magritek Halbach system using sister plugs. The susceptibility contrast was taken as $\chi=3\text{x}10^{-6}$ and the fluid bulk relaxation time as $T_b=3$s.

Micro-porosity modelling

We calculated the 2-point correlation functions of samples A and B for both SEM resolutions and used the fine scale correlation function to find an approximate model, depicted in Fig. 3. The model structures are generated with periodic boundary conditions as 250^3 voxel grey-scale images with the model domain covering 10^3 voxels of the Xray-CT image. Local grey-scale thresholds on the model structure are used to match the desired porosity indicated by the grey scale of a micro-porous voxel in the tomogram. The total image thus is made of 25000^3 voxels at the finest scale, representing a volume of about $(2.5\text{mm})^3$ at 100nm resolution.

NMR response simulation

The explicit modelling of the dephasing of the nuclear spins requires to calculate the internal magnetic field at every point in space. The structure is stored in a hierarchical way using a distributed computing approach and the internal magnetic field is calculated using the dipole approximation. Each voxel in the fine-scale model structure either has the susceptibility of the fluid or of the solid while, for intermediate porosity large scale voxels of the tomogram, a plain weighted arithmetic average is used. The static magnetic field at a particular point in space is then calculated as a sum of contributions from different scales. In particular, we do not assume that only the shortest length scale across pores or micro-pores contributes to field heterogeneity. Larger structural features of the carbonate rock can generate internal mesoscopic field inhomogeneities which are neither local to pores nor are they easily eliminated by shimming, which would also have to account for the macroscopic shape of the sample. The existence of such effects has been suggested before (e.g. Arns, 2004). Sample shape and special probe geometries can easily be accounted for if so desired.

We use a random walk technique to simulate the NMR relaxation for the CPMG pulse sequence (Arns et al., 2007). At 100nm resolution for water at room temperature, the time step of the random walk is of the order of 1μs. Since the stepsize of the random walk is sufficiently small, dephasing is simulated by tracking the phase evolution of each random walk step for step (Carr and Purcell, 1954).

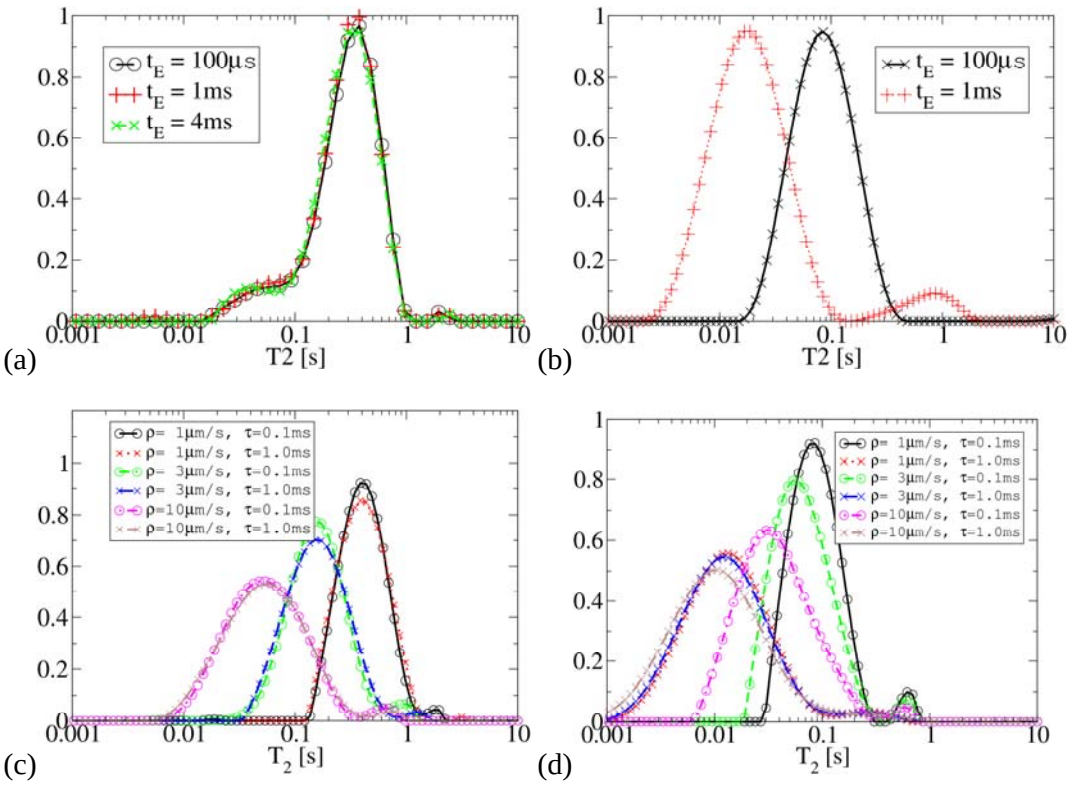

Fig. 4: Comparison of experimental and numerical NMR CPMG measurements for sample B. (a) low field (B_0=550G) and (b) high field (B_0=94000G) experiments. (c) low field and (d) high field numerical simulations for different constant surface relaxivities.

RESULTS

We show in Fig. 4 the comparison of experimental results to numerical simulations for sample B. Sample A is not shown but results are similar. From the low field experiments it is evident that the T2 distribution is not dependent on CPMG spacing for the echo spacings tested. This is also true for the simulations. The simulations were run for three different surface relaxivities, constant over the whole solid surface. A single surface relaxivity of ρ just above 1µm/s would give the best match. However, the width of the numerical T2 distribution is not as wide as the experimental one. The small T2 flank of the experimental low field curve might be due to weaker coupling and/or surface relaxivity heterogeneity. While at low field the internal field makes no contribution, the opposite is true at high field. We see a marked shift to smaller relaxation times, if the echo spacing increased. Furthermore, the numerical evaluation shows, that at high field the surface relaxivity parameter makes little difference to the T2 distribution function for larger CPMG spacings. The simulations were run with 'infinite' bandwidth of the receiver and taking all echoes including the first into account, leading to high resolution at small T2.

DISCUSSION AND CONCLUSIONS

In this paper we presented a multi-scale parallel NMR response simulator capable of simulating the full phase evolution of dephasing spins. We showed that at low field for rocks with small susceptibility contrast surface relaxivity is not arising from internal fields. At high field we demonstrate that using surface relaxivity to account for a shift in

the T2 distribution is questionable. For larger CPMG spacing the influence of surface relaxivity is neglibible, indicating the importance of internal field effects. The reversal of the importance of these two opposing effects with field strengths suggests that an intermediate regime exists where both effects are of similar order.

ACKNOWLEDGEMENTS

The authors acknowledge the member companies of the Digital Core Consortium for their support. We thank the Australian Partnership for Advanced Computing for generous allocations of computer time. This work is supported by the Australian Research Council through Discovery Grant DP0881112. We thank Michael Turner for the preparation of the SEM images.

REFERENCES

1. M.D. Hürlimann, “Effective Gradients in Porous Media Due to Susceptibility Differences”, Journal of Magnetic Resonance (1998) 131, 232-240.
2. J.L. Shafer, D. Mardon, and J. Gardner, “Diffusion effects on NMR Response of Oil & Water in Rock: Impact of Internal Gradients”, (1999) International Symposium Proceedings, Society of Core Analysts, paper SCA-9916.
3. K.-J. Dunn, “Magnetic susceptibility contrast induced field gradients in porous media”, Magnetic Resonance Imaging (2001) 19, 439-442.
4. K.-J. Dunn, M. Appel, J.J. Freeman, J.S. Gardner, G.J. Hirasaki, J.L. Shafer, and G. Zhang,”Interpretation of restricted diffusion and internal field gradients in rock data”, (2001), SPWLA 42nd Annual Logging Symposium, June 17-20, paper AAA.
5. C. H. Arns, F. Bauget, A. Ghous, A. Sakellariou, T. J. Senden, A. P. Sheppard, R. M. Sok, W. V. Pinczewski, J. Kelly, and M. A. Knackstedt; Digital core laboratory: Petrophysical analysis from 3D imaging of reservoir core fragments, Petrophysics, (2005) 46(4), 260-277.
6. C.H. Arns, A.P. Sheppard, R.M. Sok, and M.A. Knackstedt, “NMR petrophysical predictions on digitized core images”, Petrophysics, (2007) 48(3), 202-221.
7. P.A. Crossley, L.M. Schwartz, and J.R. Banavar, “Image-based models of porous media: Application to vycor glass and carbonate rocks”, Applied Physics Letters, (1991) 59(7), 3553-3555.
8. B. Biswal, P.E. Oren, R.J. Held, S. Bakke, and R. Hilfer, “Stochastic multiscale model for carbonate rocks, Physical Review E, (2007) 75, 061303.
9. K. Wu, A. Ryazanov, M.I.J. van Dijke, Z. Jiang, J. Ma, G.D. Couples, and K.S. Sorbie, “Validation of methods for multi-scale pore space reconstruction and their use in prediction of flow properties of carbonate”, (2008) International Symposium of the Society of Core Analysts, Abu Dhabi, paper SCA2008-34.
10. A.P. Roberts, “Statistical reconstruction of three-dimensional porous media from two-dimensional images”, Physical Review E, (1997) 56, 3203-3212.
11. C.H. Arns, M.A. Knackstedt, and K.R. Mecke, “Characterisation of irregular spatial structures by parallel sets and integral geometric measures”, Colloids and Surfaces A, (2004) 241, 351-372.
12. C. H. Arns; A comparison of pore size distributions derived by NMR and Xray-CT techniques, Physica A, (2004) 339(1-2), 159-165.
13. H. Y. Carr and E. M. Purcell, “Effects of diffusion on free precession in nuclear magnetic resonance problems”, Physical Review, (1954) 94, 630-642.